6. G. Goubau, Surface waves and their application to transmission lines, J Appl Phys 21 (1950), 1119–1128.
7. G. Goubau, Single-conductor surface wave transmission lines, Proc IRE 39 (1951), 619–624.
8. P. Troughton, Measurement techniques in microstrip, Electron Lett 5 (1969), 25–26.
9. P.A. Bernard and J.M. Gautray, Measurement of dielectric constant using a microstrip ring resonator, IEEE Trans Micro Theory Tech 39 (1991), 592–595.
10. A.O. Salman, D. Dibekci, S.P. Gavrilov, and A.A. Vertiy, The radiation properties of a novel wire antenna for the security fence radar, IEEE Trans Antennas Propag 56 (2008), 2852–2864.

DESIGN OF AN ON-GLASS VEHICLE ANTENNA USING A MULTILOOP STRUCTURE

Seungbeom Ahn,[1] Seulgi Park,[2] Yongho Noh,[3] Dongwook Park,[1] and Hosung Choo[1]
[1] School of Electronic and Electrical Engineering, Hongik University, 72-1 Sangsu-dong, Mapo-gu, Seoul 121-791, Korea; Corresponding author: hschoo@hongik.ac.kr
[2] Electronic Warfare R&D Center, LIG Nex1 Co., Ltd, 120-18 Mabuk-dong, Giheung-gu, Yongin 446-716, Korea
[3] Corporate Research & Development Division, Hyundai-Kia Motors, 772-1 Jangduk-dong, Hwaseong 445-706, Korea

Received 3 April 2009

ABSTRACT: *We propose a novel on-glass antenna with a multiloop structure for FM radio reception in a recreational vehicle (RV). The proposed antenna consists of multiple loops that are printed on a quarter glass with copper striplines. In spite of its simple planar structure, the antenna provides a broad matching bandwidth and a high vertical radiation gain. Antenna performances such as the return loss and boresight gain were measured after the antenna was installed in a commercial RV. The proposed on-glass antenna exhibits an average gain of about −9.5 dBi with a deviation of <4 dB compared with the gain of a conventional λ/4 roof-mounted monopole. Transparency of the antenna body was also improved by adjusting the stripline widths based on the induced current distribution.* © 2009 Wiley Periodicals, Inc.
Microwave Opt Technol Lett 52: 107–110, 2010; Published online in Wiley InterScience (www.interscience.wiley.com).
DOI 10.1002/mop.24836

Key words: *on-glass antenna; multiloop structure; FM radio band*

1. INTRODUCTION

The monopole-type antennas such as the conventional $\lambda/4$ monopole, tuned monopole, and roof-mounted microantenna have been widely used for FM radio reception in various types of vehicles [1]. These antennas, however, suffer from lack of durability and undesirable appearance as they protrude from the vehicles. To mitigate these problems, on-glass antennas printed directly on the rear or quarter glasses of a vehicle have been developed and are now commonly applied in many commercial vehicles [2–4]. The on-glass antennas, however, usually possess a relatively low vertical gain and narrow bandwidth, and exhibit nulls in their radiation patterns because they are placed in close proximity to the conducting frame of the vehicle and are printed on lossy dielectric glasses.

In this article, we propose a novel on-glass antenna that possesses a broadband characteristic and a high radiation efficiency, which makes it suitable for use in a commercial recreational vehicle (RV). The proposed multiloop structure broadens the operating band by efficiently using the given space of the quarter glass and raises the vertical gain by maximizing the z-directed currents. The multiloop structure is designed to be placed along the conducting frame of the vehicle so that it has the added benefit of a superior field of view compared with other types of glass antennas. In addition, by adjusting the widths of the striplines based on the induced current distribution, the antenna's structure can be made visually less obtrusive. The proposed on-glass antenna was built and mounted on a commercial RV, and the performance criteria such as the matching bandwidth and boresight gain were measured and compared with those of a conventional $\lambda/4$ monopole and a commercial microantenna mounted on the roof of the RV. We also measured the azimuth radiation pattern to investigate the omnidirectional property, which revealed a gain deviation of <20 dB. These results verify that the proposed antenna is superior to the commercial roof-mounted microantenna in many aspects and thus is quite suitable for a commercial RV.

2. ANTENNA STRUCTURE AND OPTIMIZATION

Figure 1 shows the proposed on-glass antenna's structure to be placed on the side frame of the back seat. The antenna consists of a conducting stripline ($\sigma = 5.7 \times 10^7$ S/m) printed on the glass ($\varepsilon_r = 7$, $\tan\delta = 0.03$ at 100 MHz) and fed by a coaxial cable ($Z_o = 50\ \Omega$) from the upper left corner of the quarter glass. To make the best use of the window's limited area and to maximize the broadband characteristics, radiation efficiency, and vertical gain, we used a multiloop structure consisting of three loops of different sizes with a common feed line. The design parameters as given by the locations of the key points, each with coordinates (x_n, y_n, z_n), determine the geometry of the three loops in the quarter glass. The multiloop structure provides a broadband operation because each loop resonates at a different frequency (at which its perimeter is approximately equal to one-half of the wavelength). Therefore, the perimeter of each loop should be carefully determined so that the entire FM radio band (80–110 MHz) is covered by the collective multiloop structure. The outer loop (perimeter of about 2 m) and the inner loop (perimeter of about 0.9 m) are designed to resonate at the lowest frequency of about 80 MHz and at the highest frequency of about 130 MHz, respectively. The middle loop (perimeter of about 1.4 m) is designed to have a resonance in the center of the FM band so as to lower the relatively high impedance of the inner and outer loops. More importantly, the middle loop can also be tuned to play a critical role in increasing the vertical

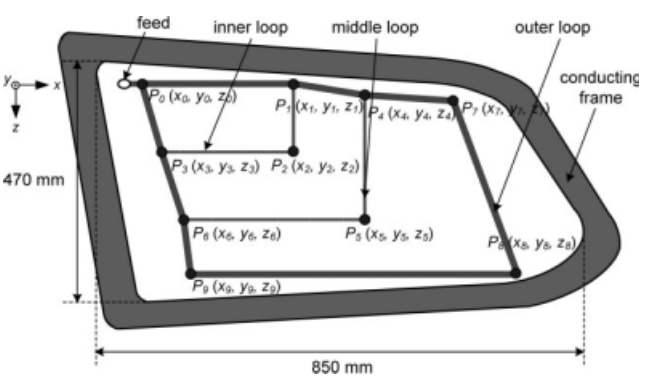

Figure 1 Geometry of the proposed on-glass glass antenna

TABLE 1 Dimensions of The Optimized Antenna (see Fig. 1)

Coordinates (mm)	$P_0(x_0, y_0, z_0)$	$P_1(x_1, y_1, z_1)$	$P_2(x_2, y_2, z_2)$	$P_3(x_3, y_3, z_3)$	$P_4(x_4, y_4, z_4)$
	(0, 0, 0)	(299, 0, 0)	(299, 69, 138)	(39, 69, 138)	(439, 13, 25)
	$P_5(x_5, y_5, z_5)$	$P_6(x_6, y_6, z_6)$	$P_7(x_7, y_7, z_7)$	$P_8(x_8, y_8, z_8)$	$P_9(x_9, y_9, z_9)$
	(439, 136, 272)	(83, 136, 272)	(615, 18, 35)	(747, 196, 392)	(100, 196, 392)
Stripline widths (mm)		$\overline{P_0P_1}, \overline{P_1P_4}, \overline{P_4P_7}, \overline{P_7P_8}, \overline{P_8P_9}, \overline{P_6P_9}, \overline{P_3P_6}, \overline{P_0P_3}$			1 mm
		$\overline{P_1P_2}, \overline{P_2P_3}, \overline{P_4P_5}, \overline{P_5P_6}$			0.3 mm

gain. When the operating frequency is higher than the dominant resonance of a typical loop antenna, a harmonic mode is created which usually decreases the vertical gain due to the cancellation of perpendicular currents. The middle loop in our proposed antenna partially suppresses the harmonic component of the outer loop and leading to an increase in the vertical gain of the antenna.

To optimize the proposed antenna's performance, the design parameters [bend points (P_0–P_9)] were determined by using a genetic algorithm (GA) in conjunction with FEKO software [5–8]. For an accurate estimation of the antenna performance, the entire vehicular structure was modeled as 3300 piecewise meshes in the simulation. In the GA optimization process, the final design goal was set to achieve a high vertical gain in the FM radio band, wherein the fitness function was defined as:

$$\text{Fitness} = \min_{\text{freq}}\{\text{Gain}(\theta = 90^{\circ}, \phi = 270^{\circ})\}. \quad (1)$$

The design goal was to maximize the fitness function, which represents the minimum gain along the boresight direction ($\theta = 90^{\circ}$, $\phi = 270^{\circ}$) in the frequency range from 80 to 110 MHz. The optimized design parameters obtained by using the GA based on the fitness function are shown in Table 1. The optimized antenna occupies an area of 850 × 470 mm^2. Because the on-glass antenna should obstruct passengers' view as little as possible, we applied a further design step to improve antenna transparency based on the simulated current distribution. The scheme is to adjust the width of the stripline based on the amount of current flowing in the stripline. Thus, 1-mm width was used for the outer loop (average current $I_{\text{avg.}} \geq -30$ dBA), and 0.3-mm width was chosen for the inner and the middle loops (average current $I_{\text{avg.}} \leq -40$ dBA). This was done to improve the transparency without significantly increasing the conducting loss of the stripline.

3. MEASUREMENT AND ANALYSIS

To verify the simulated antenna performance, the proposed antenna was built on the quarter glass of 2006 KIA Grand Carnival, and its characteristics were measured in a semianechoic chamber [9]. Figure 2 shows the measured and simulated return loss of the proposed antenna. The measurement was performed using an Agilent E5071A network analyzer with an ETS-Lindgren 3121C dipole as the transmitter in a semianechoic chamber of dimensions 30 × 30 m^2 [10]. The result shows a 3-dB bandwidth of 8.5% (from 90 to 98 MHz), which agrees fairly well with the simulation result. Figure 3 represents the measured boresight gain of the proposed antenna (solid line) installed on a commercial RV. In the same figure, the measurement for a conventional $\lambda/4$ monopole (height = 75 cm, dash-dotted line) and a commercial microantenna (height = 20 cm, dotted line) mounted on the same vehicle roof were plotted for comparison. Our proposed antenna shows a boresight gain of more than −15 dBi in the entire FM radio band with an average gain of −9.67 dBi, which is superior to that of the microantenna by more 10 dB on an average, and approaches the gain of the conventional $\lambda/4$ monopole, which has a deviation of about 3.5 dB on an average. We also measured the boresight gain of the antenna (dashed line) without adjusting the stripline widths (fixed stripline width of 1 mm). The result shows that the proposed antenna has almost the same boresight gain (the discrepancy <1 dB on average) as the design using the fixed stripline width, even though the transparency of the antenna has been greatly enhanced. To examine the omnidirectional property of the antenna, we measured the azimuth radiation pattern of the proposed antenna. As shown in Figure 4, the maximum radiation gain occurs at the boresight direction of 270° and the average gain exceeds −15 dBi at 90, 100, and 110 MHz, with the maximum difference in the gain at these frequencies being <20 dB.

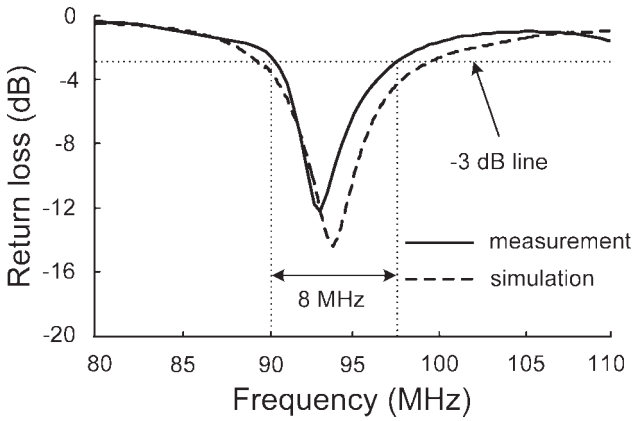

Figure 2 Measured (——) and simulated (------) return loss of the proposed antenna

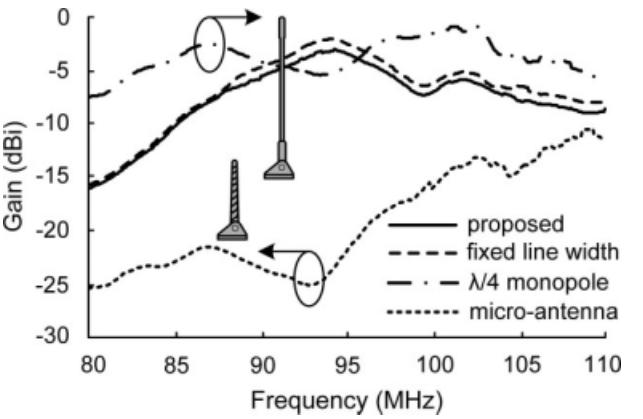

Figure 3 Measured gain (——) of the proposed antenna, measured gain (------) of the antenna with the fixed stripline width, measured gain (– · – · –) of the $\lambda/4$ conventional monopole, and measured gain (……) of the roof-mounted microantenna

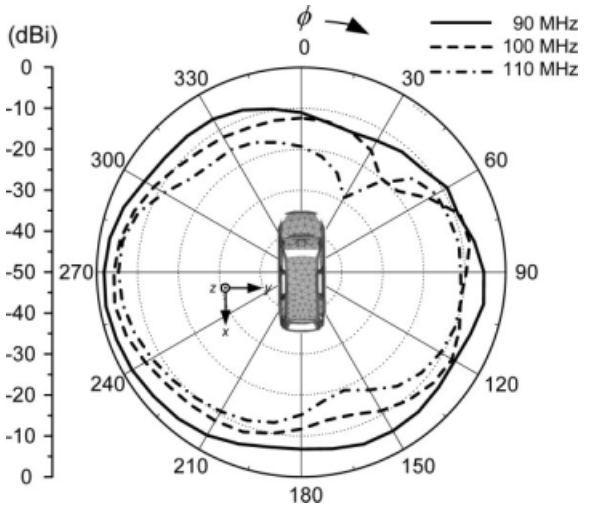

Figure 4 Measured radiation pattern of the proposed antenna

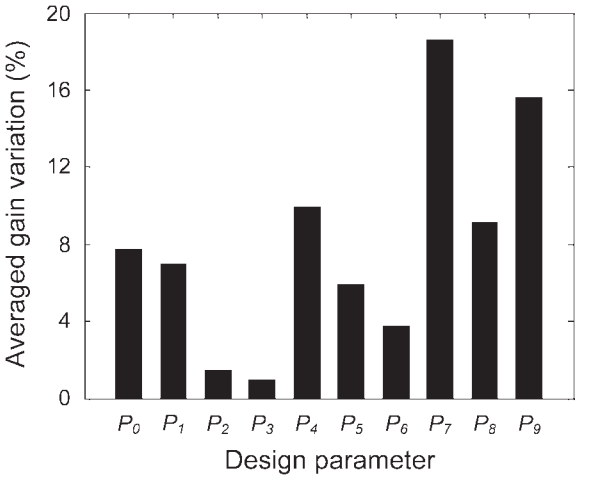

Figure 6 Averaged gain variation: gain sensitivity with respect to perturbations

To explain the operating principle of the proposed on-glass antenna and to demonstrate its broadband matching characteristics from the circuit point of view, we developed a circuit model for the antenna as shown in the inset of Figure 5. The circuit model consists of three resonance circuits resonating at 80.3, 111, and 135.5 MHz, respectively. The values for the lumped elements in the circuit model are found by data fitting: $R_1 = 3000\ \Omega$, $L_1 = 170$ nH, $C_1 = 23$ pF, $R_2 = 160\ \Omega$, $L_2 = 15$ nH, $C_2 = 137$ pF, $R_3 = 2450\ \Omega$, $L_3 = 78$ nH, and $C_3 = 18$ pF. The impedance for the equivalent circuit model (solid line) agrees well with the corresponding result obtained from the electromagnetic simulation of the proposed antenna structure (dashed line). The proposed antenna is suitable for broadband matching (to 50 Ω) because the resonance of the middle loop adjusts the high resonance impedances of the inner and outer loops. As a result, the resistance of the antenna's input impedance is in the range of 25–60 Ω and the reactance remains close to 0 Ω from 90 to 110 MHz.

To estimate the sensitivity of the antenna performance with respect to possible manufacturing errors, we performed a perturbation analysis. Figure 6 shows the averaged gain variation in the simulation due to a slight change in the location for each bend point (P_0–P_9). The averaged gain variation was obtained by averaging the changes of gain over the operating frequency range when each bend point is shifted by 10 mm in four different directions (up, down, left, and right) from its original location. It is defined as follows:

$$\text{Averaged gain variation}(\%) = \frac{1}{4N}\sum_{i}^{N}\sum_{j}^{4}\left|\frac{G_{\text{ori}}(f_i) - G_{\text{shift}}(L_j, f_i)}{G_{\text{ori}}(f_i)}\right| \times 100 \quad (2)$$

where L_j represents a 10-mm perturbation of the bend points under consideration in the j-th direction ($j = 1$–4 for up, down, left, and right, respectively) and f_i is the i-th frequency out of the 61 discrete frequencies ($N = 61$) spanning the 80–110 MHz band. The largest averaged gain variations were observed at bend points in the outer loop (P_7, P_8, and P_9), followed by bend points in the middle loop (P_4, P_5, and P_6). This result seems to indicate that the inner loop is least sensitive and the outer loop is most sensitive to errors arising from misplacement of the bend points.

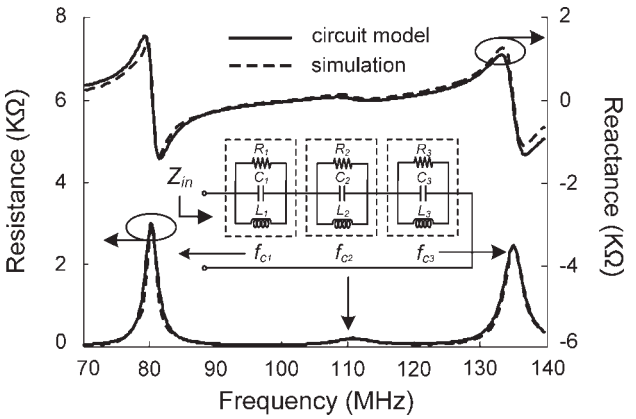

Figure 5 The equivalent circuit model of the proposed glass antenna

4. CONCLUSIONS

In this article, we proposed a novel on-glass antenna with a printed multiloop structure. The antenna built according to the design exhibits an average boresight gain of −9.67 dBi across the entire FM radio frequency range, which is about 10 dB higher than the gain of a commercial roof-mounted microantenna. The transparency of the antenna can also be greatly enhanced by adjusting the stripline widths. These results verify that the proposed on-glass antenna is suitable for FM radio reception in a commercial RV.

ACKNOWLEDGMENT

This study was supported by Hyundai-Kia Motors and the IT R&D program of MKE/IITA. [2009-F-042-01, A Study on Moblie Communication System for Next-Generation Vehicles with Internal Antenna Array].

REFERENCES

1. K. Fujimoto and J.R. James, Mobile antenna system handbook, 2nd ed., Artech House, Massachusetts, 2001.
2. R. Abou-Jaoude and E.K. Walton, Numerical modeling of on-glass conformal automobile antennas, IEEE Trans Antennas Propag 46 (1998), 845–852.
3. Y. Noh, Y. Kim, and H. Ling, Broadband on-glass antenna with meshgrid structure for automobiles, Electron Lett 41 (2005), 1148–1149.

4. J.C. Batchelor, R.J. Langley, and H Endo, On-glass mobile antenna performance modeling, IEE Proc Microwave Antennas Propag 148 (2001), 233–238.
5. D.E. Goldberg, Genetic algorithms in search, optimization and machine learning, Addison-Wesley, Reading, MA, 1989.
6. Y. Rahmat-Samii and E. Michielssen, Electromagnetic optimization by genetic algorithms, Wiley, New York, 1999.
7. T. Hiroyasu, M. Miki, and S. Watanabe, The new model of parallel genetic algorithm in multi-objective optimization problems—Divided range multi-objective genetic algorithm, Proc Congr Evol Comput 1 (2000), 333–340.
8. EM Software & Systems–S.A. (Pty) Ltd., FEKO suite 5.3, EM Software and Systems, Stellenbosch, 2007.
9. 2006 KIA Grand Carnival. Available at: http://www.kia.co.kr.
10. Transmit antenna. Available at: http://www.ets-lindgren.com/manuals/3121C.pdf.

X-BAND HIGH-POWER AMPLIFIER WITH A MAGNETICALLY COUPLED POWER-COMBINER

Kyung-Ai Lee, Changkun Park, Jong-Hoon Chun, and Songcheol Hong
School of Electrical Engineering & Computer Science, Division of Electrical Engineering, Korea Advanced Institute of Science and Technology, 373-1 Guseong-Dong, Yuseong-Gu, Daejeon 305-701, Republic of Korea; Corresponding author: schong@ee.kaist.ac.kr

Received 9 April 2009

ABSTRACT: *In this article, a high-power amplifier for X-band application is studied, which consists of a two-stage amplifier with magnetically coupled power-combiners and dividers. These are based on transmission line transformers, which has lower loss characteristics than spiral-type transformers at the frequencies. The proposed amplifier utilizes the voltage-combining concept with the transformers and differential amplifiers. The size of the amplifier is also minimized by using the virtual grounds of the differential structure. The saturated output power of the power amplifier is 38.1 dBm (6.45 W), and the gain is 17 dB at 10 GHz. The area of the chip is 2.56 mm × 3.13 mm and the power density of the amplifier is 806 mW/mm^2.* © 2009 Wiley Periodicals, Inc. Microwave Opt Technol Lett 52: 110–113, 2010; Published online in Wiley InterScience (www.interscience.wiley.com). DOI 10.1002/mop.24851

Key words: *X-band power amplifier; tournament shaped; voltage combiner; binary combiner*

1. INTRODUCTION

Currently, there is an increasing demand for X-band radar T/R modules for military and public services use. One of the most important components of the module is a high-power amplifier, which should preferably be developed as a microwave monolithic circuit (MMIC) for the minimization and reproducibility of the module [1–4]. The conventional amplifiers have their transistors arranged in a row using binary-tree-combining topology. With this topology, the summed output power is delivered to an output load by means of the power-combining.

Figure 1 shows an example of a binary-combining topology. Mostly, an output impedance of a power transistor ($R1$) is lower than 50 Ω, which needs matching components like inductors and capacitors. These lumped devices have large power losses. To solve this problem, the voltage-combining topology has been studied with CMOS technology at a frequency band lower than

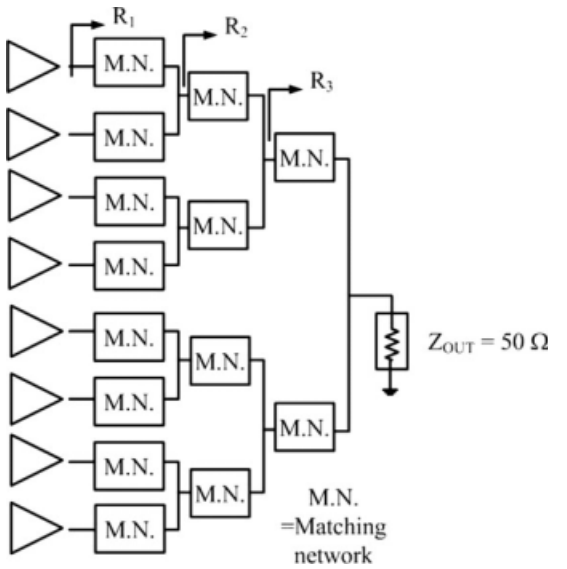

Figure 1 The binary-combining topology with eight transistors

5 GHz [5, 6]. In this topology, the magnetically coupled lines substituted the inductors and capacitors (Fig. 2). If the magnetically coupled lines work well in X band, these help to reduce the power loss of the power-combiner. The differential structures in the topology have virtual grounds, which eliminate $\lambda/4$ drain bias lines. The concept of combining voltage is therefore introduced to improve the performance and to reduce the size of the high-power amplifier.

This paper describes the performance of the high-power amplifier at X band with the magnetically coupled power-combiner, which utilizes the voltage-combining concept. The concept of the voltage-combining was introduced with distributed active transformer [6], but it cannot be adopted in GaAs technology, where the gate must be aligned to the same direction. This is because it utilized the circular geometry to implement the power-combining and the output matching simultaneously. Therefore, the tournament-shaped magnetically coupled power-combiner is used for X-band high-power amplifier.

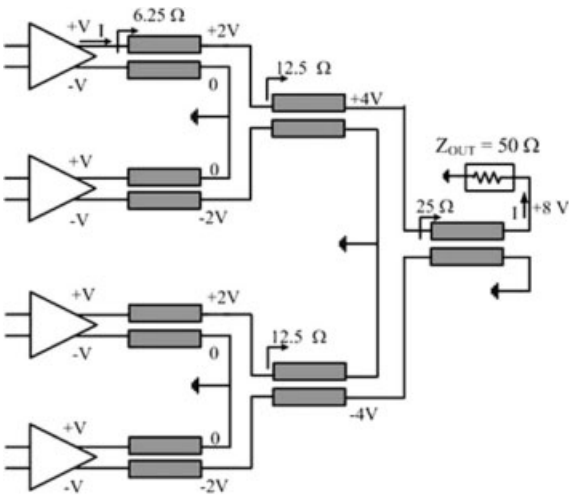

Figure 2 The voltage-combining topology with eight transistors